ACS APPLIED MATERIALS & INTERFACES

Research Article

www.acsami.org

A Li–O_2/Air Battery Using an Inorganic Solid-State Air Cathode

Xiaofei Wang, Ding Zhu, Ming Song, Shengrong Cai, Lei Zhang, and Yungui Chen*

College of Materials Science and Engineering, Sichuan University, Chengdu 610065, China

Supporting Information

ABSTRACT: The "(−) lithium (Li) anodelorganic anolyte + inorganic catholytel solid-state cathode (+)" Li–O_2/air battery based on an inorganic solid-state air cathode was fabricated with a simple method. The electrochemical performance and reaction products of the Li–O_2/air batteries under pure O_2 and ambient air were investigated, respectively. The inorganic Li-ion conductive solid-state electrolyte $Li_{1.3}Al_{0.3}Ti_{1.7}(PO_4)_3$ was stable during cycling and avoided the decomposition and volatilization problems that conventional organic electrolytes faced. Moreover, the porous air cathode provided a sufficient gas-phase O_2-transport channel, facilitating the achievement of a high capacity of 14192 or 7869 mA h g^{-1} under pure O_2 or ambient air, respectively. Our results demonstrate that the Li–O_2/air battery using an inorganic porous air cathode has a great potential for practical application.

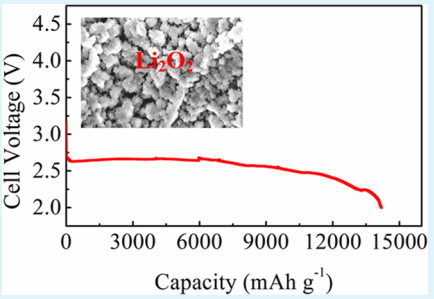

KEYWORDS: *Li–O_2/air battery, solid-state electrolyte, Li_2O_2, LATP, electrochemical performance*

1. INTRODUCTION

The development of large-scale energy devices, such as plug-in hybrid electric vehicles (PHEVs) or electric vehicles (EVs), is the trend in the future.[1] However, the typical energy density of today's lithium (Li)-ion battery is between just 100 and 200 W h kg^{-1}, which is too low to meet the demand of practical PHEVs or EVs (700 W h kg^{-1}).[2] The Li–O_2/air battery has attracted much attention as a potential power system because of its ultrahigh theoretical energy density.[3] Different from a Li-ion battery, oxygen (O_2), the cathode active material of a Li–O_2/air battery, is not stored in the battery but comes from air. The energy density of a Li–O_2/air battery is about 10 times higher than that of a Li-ion battery.[4,5] Despite its great promise, there are still many critical drawbacks to developing a practical Li–O_2/air battery.

For much research on Li–O_2/air batteries based on organic liquid electrolytes, the flowing nature of the organic liquid electrolytes will flood the O_2-transport channel and the oxygen solubility and diffusion ability in the organic liquid electrolytes are very slow, which severely limit the reaction kinetics at the electrolyte/carbon interface.[6] Our previous research on an organic-based electrolyte Li–O_2 battery demonstrated the importance of the availability of O_2, which even required intermittent operation to improve the discharge performance.[7] Moreover, the discharge performance of the organic-based electrolyte Li–O_2 battery seriously deteriorated when the working environment was altered to ambient air; we found that the typical capacity under ambient air was less than 1 in 10 of the capacity under pure O_2.[8] Besides, two problems inevitably arise:[9−14] (1) Organic liquid electrolytes commonly used are unstable and easily decomposed by the superoxide ion via nucleophilic attack. (2) Organic electrolytes commonly used will inevitably react with the discharge product, Li_2O_2. All of the problems mentioned above limit its practical application.

Solid-state Li-ion conductors are very stable and have acceptable Li-ion conductivity, which provide a new way to solve these problems.[15] Polyplus successfully coated the Li metal with a solid ceramic membrane, which kept the Li chemically isolated but allowed it to be electrochemically active; the protected Li electrode could even work in water. These kinds of ceramic materials, such as Li–Al–Ge–PO_4 (LAGP) and Li–Al–Ti–PO_4 (LATP), have received considerable attention as electrolytes for various types of Li–O_2 batteries.[2,16−19] Recently, many excellent studies have been made to improve the performance of a solid-state Li–O_2/air battery. Kichambare et al. made great efforts to improve the performance of the solid-state, rechargeable Li–O_2 battery and achieved superior performance by fabricating the cathode with N–C and LAGP.[20] Zhou's group reported a series of excellent works by introducing C and LATP.[21,22] The reported methods expanded the range of the solid-state Li–O_2/air battery. However, there are still many challenges before practical application is realized, for example, improving the capacity (especially under ambient air), lowering the cost, and simplifying the preparation process.

In this paper, the solid-state Li–O_2/air battery based on a porous inorganic solid-state air cathode was fabricated with a simple method, which has the following advantages: (1) Minimize the O_2-transport limit faced by traditional organic electrolytes. (2) Make the battery able to directly work in ambient air. (3) Given a sufficient amount of Li metal anode, the reasonable and simply designed battery will be able to mechanically discharge by replacing the used cathode with a new cathode. The proposed Li–O_2/air battery achieved high capacity without using any catalyst to promote the oxygen

Received: March 5, 2014
Accepted: June 24, 2014
Published: June 24, 2014

   dx.doi.org/10.1021/am501315n | ACS Appl. Mater. Interfaces 2014, 6, 11204−11210

reduction and oxygen evolution reactions, indicating that the solid-state air cathode has a great potential for development.

2. EXPERIMENTAL SECTION

2.1. LATP Synthesis. A solid-state Li-ion conductor of $Li_{1.3}Al_{0.3}Ti_{1.7}(PO_4)_3$ was synthesized according to previous reports.[23−25] Stoichiometric amounts of Li_2CO_3, Al_2O_3, TiO_2, and $(NH_4)H_2PO_4$ were ball-milled in ethanol for 30 min and then dried by distillation; the dried powder was heated at 400 °C for 2 h to release volatile products before the temperature was raised to 800 °C and held at that temperature for 2 h in air. The obtained LATP was ball-milled to ∼50 μm, and the powder was cold-pressed into sheets and sintered at 800 °C for 4 h in air. The thickness of the obtained LATP sheets was measured to be around 300 μm, and the diameter was 1.8 cm.

2.2. Fabrication of the Porous Air Cathode. The porous air cathodes were made of Super P conductive carbon black (SP), poly(vinylidene fluoride), and LATP in weight ratios of 10:5:85. The Brunauer−Emmett−Teller surface area of SP is demonstrated to be 780.5 $m^2\ g^{-1}$. SP is a kind of spherical particle, and the pore surface of SP is 91.7 $m^2\ g^{-1}$. The mixture was milled by hand in an agate mortar, and *N*-methyl-2-pyrrolidone (NMP) was dropwise added to form a slurry mixture and then ultrasound-dispersed evenly. The air cathode was prepared by hand-painting the slurry mixture onto a nickel (Ni) foam current collector with a diameter of 1.4 cm. SP provides the electron conductivity and reactive active sites, and LATP provides the Li-ion conductivity. The prepared air cathode was dried at 120 °C under vacuum for 12 h to remove the residual NMP. The loading area was about 1.5 cm^2, the as-obtained air cathode had a loading weight of SP of 0.67 mg cm^{-2}, and the porosity of the cathode materials was about 43.7%.

2.3. Battery Assembly. The proposed Li−O_2/air battery "(−) Li anode|organic anolyte + inorganic catholyte|solid-state cathode (+)" was assembled in an argon-filled glovebox (Chengdu Dellix Industry Co., Ltd.); the schematic diagram of the Li−O_2/air battery is shown in Figure 1.

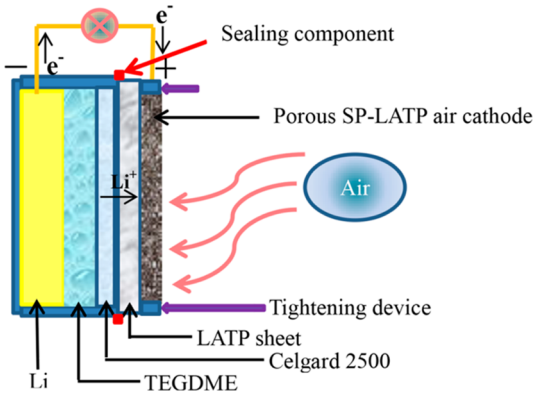

Figure 1. Schematic diagram of the proposed Li−O_2/air battery.

At the side of Li metal (1.6 cm diameter), an organic electrolyte of 0.9 M lithium bis(trifluoromethanesulfonyl)imide (purchased from Aladdin Reagent, 99%) in tetraethylene glycol dimethyl ether (TEGDME; purchased from Aladdin Reagent, 99%) was introduced to wet the Li metal and LATP sheet and served in the role of decreasing the interface impedance; a Celgard 2500 membrane (1.6 cm diameter) was used to separate the Li metal and LATP sheet because Li reacts easily with LATP when contacted directly.[26] Using an O-ring as the sealing component and making sure that no gas residue among the Li/Celgard 2500/LATP sheet and no electrolyte leak out, all components were sealed together compactly to make a Li−O_2/air battery. The configuration of the Li−O_2/air battery and assembly details are shown in the Supporting Information (SI; Figure S1). The TEGDME-based organic electrolyte Li−O_2 battery without the LATP sheet was assembled according to the same fabrication process, and 400 μL of electrolyte was added to immerse the air cathode.

2.4. Electrochemical Measurement. Electrochemical tests were carried out at room temperature using a LAND tester (CT2001A, Wuhan LAND Electronic Co., Ltd.). After standing for at least 2 h, the battery was discharged and charged. The current density and capacity were normalized by the weight of SP. The operating environment involved a pure O_2 atmosphere (1 atm) and an ambient air environment (0.945 atm and relative humidity = 70%). Electrochemical impedance spectroscopy (EIS) was carried out using a PARSTAT 2273 instrument (Princeton Applied Research), and spectra were obtained in the frequency range from 10 kHz to 10 mHz with an alternating-current (ac) amplitude of 5 mV.

2.5. Microstructure Characterization. X-ray diffraction (XRD) was carried out using a Dandong DX-2600 diffractometer with Cu Kα radiation and a power of 35 kV × 25 mA at a scan rate of 0.04° s^{-1}. Before XRD test was done, the cathode of the Li−O_2 battery was sealed in a packet to avoid the influence of ambient air. Attenuated total reflectance Fourier transform infrared (ATR-FTIR) measurements for the cathodes were carried out to identify the discharge product on a Nicolet 6700 spectrometer (Thermo Fisher Scientific). The micrograph was investigated with scanning electron microscopy (SEM) analysis using a JSM-7500F scanning microscope. X-ray photoelectron spectroscopy (XPS) was carried out to identify the stability of LATP using XSAM-800 (KRATOS).

3. RESULTS AND DISCUSSION

3.1. Phase and Li-Ion Conductivity of LATP. Figure 2a shows the XRD pattern of the obtained LATP powder. A pure

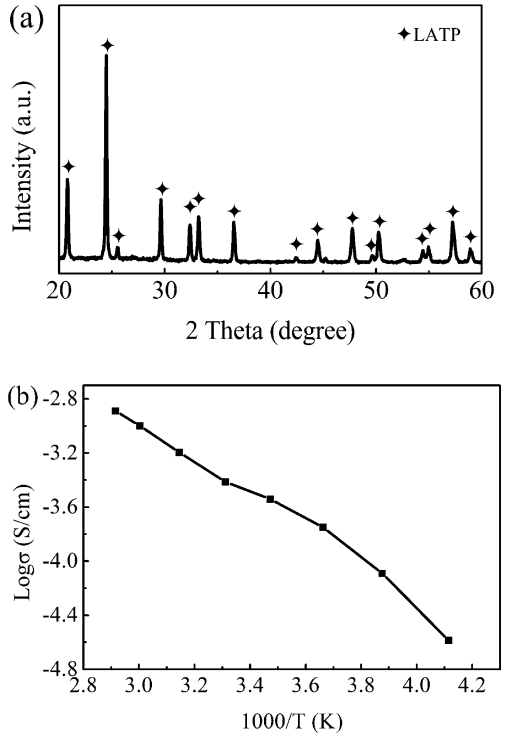

Figure 2. (a) XRD pattern. (b) Arrhenius curve of the synthetic LATP.

NASICON-type phase is indicated, the XRD pattern is in agreement with that of $LiTi_2(PO_4)_3$ (JCPDF card no. 35-0754), and no any impure phases could be found as Al^{3+} ions replaced Ti^{4+} ions. Figure 2b shows the Arrhenius curve of the synthetic LATP ceramic electrolyte tested in the range of 243−343 K. The plot of log σ against 1000/T was found to be linear, and

the Li-ion conductivity of the LATP sheet at 30 °C was 3.8 × 10^{-4} S cm^{-1}.

3.2. Electrochemical Performance of the Solid-State Li−O_2/Air Battery. The assembled solid-state Li−O_2 battery was first operated under pure O_2. Figure 3a shows the first discharge/charge curves of the Li−O_2 battery at the current density of 100 mA g^{-1} between 2.0 and 4.5 V (vs Li^+/Li). It was inspiring to find that the battery showed typical voltage but high capacity. The initial discharge voltage was about 2.65 V; at the discharge terminal, the capacity reached 14192 mA h g^{-1} (red line) and the recharge capacity reached 11473 mA h g^{-1} (blue line). XRD characterization was carried out to characterize the discharge products: the peaks related to Li_2O_2 (JCPDF card no. 73-1640) are clearly evident, and no significant LiOH and Li_2CO_3 peaks could be detected, as shown in Figure 3b. The Li_2O_2 peaks were rarely observed after recharging to 4.5 V, indicating that the recharging process made Li_2O_2 decompose. Further refined analysis of the cathodes was obtained by FTIR; the results are shown in Figure 3c. No significant Li_2CO_3 could be identified at the discharge/charge terminals. The first discharge time was nearly 6 days, excluding the possible influence of trace air contained in pure O_2. Recently, Zhang and Zhou reported excellent research on the Li−O_2 battery using a single-walled nanotube/ionic liquid gel electrolyte air cathode.[17] They charged the Li−O_2 battery to 5.0 V in order to achieve a better performance; although that is a feasible method, the Li_2O_2 peaks still existed even when charged to 5.0 V and without modification of the CNG, and the charge voltage was above 4.5 V after modification of the CNG; meanwhile, the preparation process was complex, and the cost was high. In this paper, limiting the charge voltage to 4.5 V successfully made Li_2O_2 decompose, and it was also interesting to find that the initial charge voltage was below 4.0 V and that situation was maintained for a long time. In order to explore the stability of the current collector, the cathode without SP and LATP (only Ni foam collector) was charged to 4.5 V, but no charge voltage plateau could be observed (Figure S2 in the SI); the result suggested that Ni foam was stable in our experiment. The lower charge capacity than discharge capacity was attributed to the formation and decomposition of a tiny amount of Li_2CO_3, which will be discussed later.

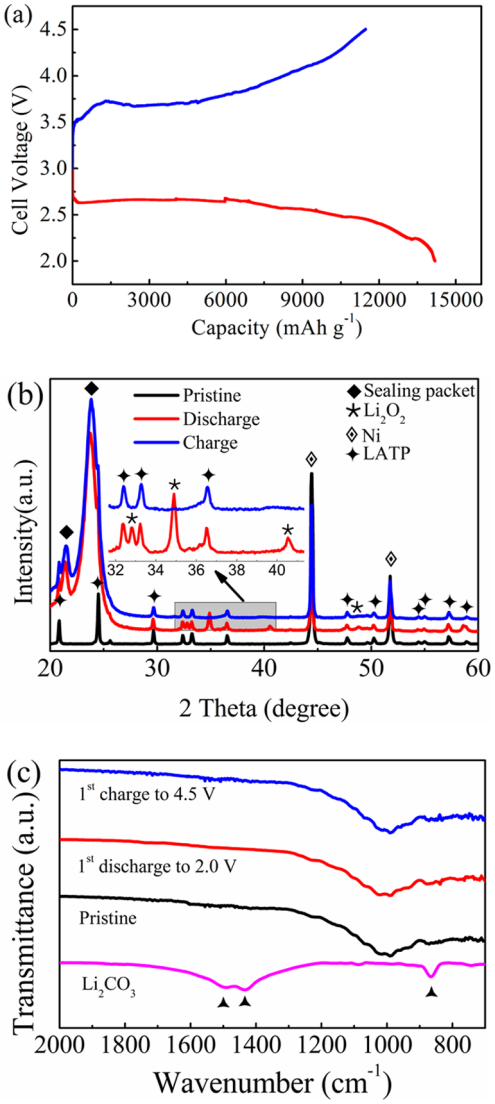

Figure 3. (a) First discharge/charge curves of the Li−O_2 battery. (b) XRD patterns of the air cathodes. Inset: partially magnified. (c) ATR-FTIR spectra of the cathodes.

Many researchers have reported the achievement of high capacity by introducing functionalized graphene sheets and carbon nanotubes or introducing various catalysts such as MnO_2,[27] perovskite oxide,[28] platinum/gold,[29] palladium,[9,30] and so on.[31−33] Herein, the mixture of SP with LATP powder that pasted on the porous Ni foam could achieve high discharge capacity (14192 mA h g^{-1} at the current density of 100 mA g^{-1}) without using any catalyst or functionalized carbon material. Meanwhile, the charge voltage was even lower than that in research on the conventional organic-based electrolyte Li−O_2 battery employing MnO_2 as the catalyst.[27] The particle size of the pristine SP was about 100 nm (not shown in the paper), but the SEM image of the air cathode after discharge revealed that Li_2O_2 particles wholly deposited onto the SP and gradually covered SP uniformly (Figure S3a in the SI), resulting in the SP particle size increasing to about 300 nm, as shown in the histogram of the diameter distribution of Li_2O_2 particles (Figure S4 in the SI). By contrast, the TEGDME-based organic electrolyte Li−O_2 battery was also assembled with the same loading weight of SP, but the energy output was only 3427 mA h g^{-1} (Figure S5 in the SI); we have reason to believe that the high capacity of the solid-state Li−O_2 battery was attributed to the sufficient available O_2; in other words, a solid-state air cathode minimizes the O_2-transport limit faced by traditional organic electrolyte, facilitating the achievement of good electrochemical performance.

To evaluate the cycling performance, the Li−O_2 battery was cycled at the same current density of 100 mA g^{-1} with a fixed capacity of 500 mA h g^{-1} in the range between 2.0 and 4.5 V (vs Li^+/Li). Figure 4a shows different discharge/charge curves with fixed capacity. The first discharge voltage was about 2.65 V (vs Li^+/Li), and the first recharge voltage was lower than that in Figure 3a because a slight amount of the discharge product (Li_2O_2) could easily be decomposed. During 14 cycles, the discharge voltage gradually decreased, especially from the 10th cycle. The cycling performance in Figure 4b also revealed that the 11th recharge capacity was incomplete and dropped to 468 mA h g^{-1}; after that, the discharge plateau dropped and inclined significantly, and the recharge capacity decayed slowly. In addition, the trend of a drop in the discharge capacity from about 4.0 V to around 2.7 V was strengthened by increasing the cycle number, which mainly came from electrochemical

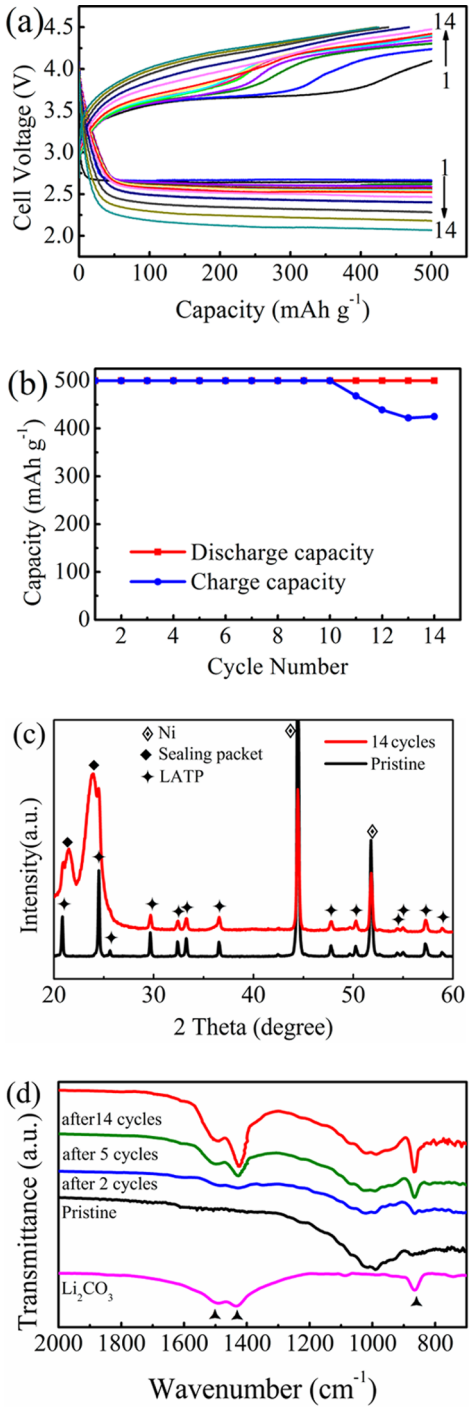

Figure 4. Electrochemical performance and characterization of the Li–O_2 battery: (a) discharge/charge curves; (b) cycling performance; (c) XRD patterns of the air cathodes; (d) ATR-FTIR spectra of the cathodes at different cycles.

polarization. It was considered that the poor cycling performance and electrochemical polarization were caused by some unfavorable side reactions; therefore, the reaction mechanism should be considered. In order to obtain further information, the cathodes were examined by XRD; the results are shown in Figure 4c. However, no significant Li_2O_2 or Li_2CO_3 peaks could be observed from the XRD patterns, and no other phase could be identified after 14 cycles. Further refined analysis of air cathodes after cycling showed the existence of Li_2CO_3, as shown in Figure 4d, examined by FTIR. A slight amount of Li_2CO_3 could be identified after 2 cycles, and clear evidence of Li_2CO_3 could be found after 5 cycles; it was deduced that the amount of Li_2CO_3 gradually increased during 14 cycles. The SEM image of the air cathode after 14 cycles revealed some new larger particles existing among the SP (Figure S3c in the SI), which was significantly different from that discharged to 2.0 V (Figure S3a in the SI). We speculated that the formed Li_2CO_3 covered the carbon surface, resulting in the observed capacity fading and increasing electrochemical polarization. In order to accurately characterize the stability of LATP, XPS spectra of LATP before and after 14 cycles were examined (Figure S6 in the SI); the peaks at higher (459.8 eV) and lower (465.3 eV) binding energies were associated with the Ti^{4+} state,[34] and no Ti^{4+} $2p_{3/2}$ and Ti^{4+} $2p_{1/2}$ binding energies shifted to lower binding energies, which certified the stability of LATP. Impedance profiles of the LATP sheet before and after cycling were also examined (see Figure S7 in the SI); it was inspiring to find that there was no significant change in the ac impedance behavior between the original and cycled sheets, so it is deduced that LATP was stable during cycling.

Many researches on Li–O_2 batteries based on organic liquid electrolytes revealed the formation of Li_2CO_3 during the electrochemical process, which was attributed to the instability and decomposition of the organic electrolyte. In this paper, LATP was stable during cycling; when the Li–O_2 battery was first discharged to 2.0 V, no significant Li_2CO_3 could be identified, and that process consumed nearly 6 days, excluding the possible influence of trace air contained in pure O_2. However, it was found in Figure 4d that Li_2CO_3 gradually accumulated in the cathode upon cycling. It has been reported that carbon was relatively stable below 3.5 V (vs Li^+/Li) upon discharge or charge but was unstable upon charging above 3.5 V, especially in the presence of Li_2O_2, causing the oxidation and decomposition reaction of carbon to form Li_2CO_3.[14,35] In this paper, Li_2CO_3 may came from the reaction of Li_2O_2 with carbon because of the inertia of Li_2CO_3, which could be decomposed only at higher voltage, making it difficult to decompose.[36] The undesirable side reaction resulted in the loss of carbon, decreasing the reactive active sites and influencing the following electrochemical properties, and eventually caused deterioration of the cycling performance. Because of the influence of Li_2CO_3 that was generated via a side reaction, the first full charge capacity was less than that of discharge.

The corrosion of the Li metal anode could be avoided with the protection of a LATP solid-state electrolyte, so the proposed Li–air battery could be directly operated under ambient air. Figure 5a shows the first discharge/charge curves of the solid-state Li–air battery at the same current density of 100 mA g^{-1} between 2.0 and 4.5 V (vs Li^+/Li). It was found that the initial discharge voltage was about 2.65 V, the same as that under a pure O_2 atmosphere, indicating that the low oxygen pressure (21% O_2 in air) did not significantly influence the discharge behavior. At the discharge terminal, the capacity reached 7869 mA h g^{-1} (red line), and at the charge terminal, the capacity reached 6234 mA h g^{-1} (blue line), as shown in Figure 5a. The discharge products under ambient air included Li_2O_2, LiOH, and Li_2CO_3, as shown in Figure 5b, which was significantly different from that of the solid-state Li–O_2 battery (Figure 3b). The byproducts came from the side reactions, once the external atmosphere altered to ambient air, H_2O, and CO_2 participated in the reactions according to the following equations:

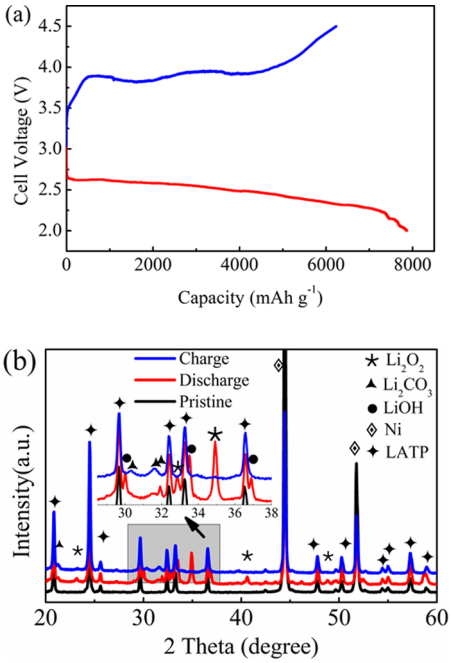

Figure 5. (a) First discharge/charge curves of the Li−air battery at the current density of 100 mA g^{-1}. (b) XRD patterns of the air cathodes. Inset: partially magnified.

$$2Li_2O_2 + 2H_2O \rightarrow 4LiOH + O_2 \quad (1)$$

$$2LiOH + CO_2 \rightarrow Li_2CO_3 + H_2O \quad (2)$$

$$2Li_2O_2 + 2CO_2 \rightarrow 2Li_2CO_3 + O_2 \quad (3)$$

Because of the side reactions, the final discharge products were clearly different from that of the solid-state Li−O_2 battery. Meanwhile, the particle size of the discharge products was irregular and larger than that operated under pure O_2 (Figure S3b in the SI); it was speculated that it is a mixture of Li_2O_2, LiOH, and Li_2CO_3. The energy output of the solid-state Li−air battery was lower than that of the solid-state Li−O_2 battery, but this value was very inspiring compared with the TEGDME-based organic electrolyte Li−air battery, whose discharge capacity was only 452 mA h g^{-1} (Figure S5 in the SI) under ambient air with the same loading weight of SP and the same current density. It is reported that the performance of the organic-based electrolyte Li−air battery deteriorated when the oxygen pressure was decreased because the oxygen solubility and diffusion ability could not meet the demand. Our results indicated that the effect of the oxygen pressure on the performance of the solid-state Li−O_2/air battery was much less than that of the organic-based electrolyte Li−O_2/air battery. A Li−air battery using a solid-state air cathode achieved O_2 via the diffusion of gas-phase O_2 in the porous air cathode, minimizing the O_2-transport limit and facilitating the achievement of good performance, which has a great potential for practical application. However, because of the contamination of H_2O and CO_2, which influenced the electrochemical performance, a decline of the energy output resulted. The first charge voltage was higher than that of the solid-state Li−O_2 battery because the byproduct Li_2CO_3 was difficult to decompose. After recharging to 4.5 V, the Li_2O_2 and LiOH peaks nearly disappeared, although the peak intensity of Li_2CO_3 had significantly decreased and partial peaks disappeared, but typical Li_2CO_3 peaks still existed, indicating that the recharge of Li_2CO_3 was incomplete.

To evaluate the cycling performance, the Li−air battery was operated at a current density of 100 mA g^{-1} with a fixed capacity of 500 mA h g^{-1}. The discharge/charge curves are shown in Figure 6a. It was found that the initial discharge curve was similar to the performance under pure O_2, but the subsequent discharge plateau dropped faster than that of the solid-state Li−O_2 battery, especially from the 8th cycle. The

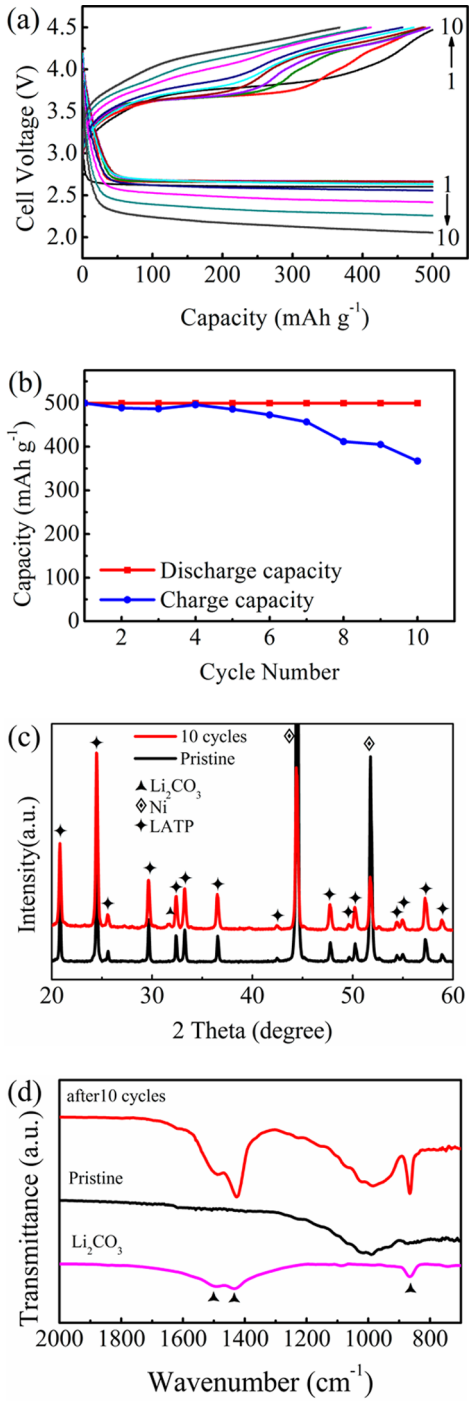

Figure 6. Electrochemical performance and characterization of the Li−air battery: (a) discharge/charge curves; (b) cycling performance; (c) XRD patterns of the air cathodes; (d) ATR-FTIR spectra of the air cathodes.

cycling performance is shown in Figure 6b; the recharge capacity was incomplete except for the first recharge. The recharge capacity decreased to 367 mA h g^{-1} after 10 cycles, and the subsequent discharge capacity also declined (not shown in this paper). After 10 cycles, the cathode of the solid-state Li–air battery was examined by XRD and FTIR, and the results are shown in parts c and d of Figure 6, respectively. One significant Li_2CO_3 peak was observed in Figure 6c, and the existence of Li_2CO_3 was clearly verified by ATR-FTIR, as shown in Figure 6d. No significant Li_2O_2 and LiOH peaks could be observed because they were easier to decompose than Li_2CO_3. The SEM image after 10 cycles revealed that the microstructure was different from that operated under pure O_2 (Figure S3d in the SI); it was speculated that the narrow and long particles were Li_2CO_3, which was associated with the capacity fade and battery death.

3.3. Discussion. Both Li–O_2 and Li–air batteries using inorganic solid-state air cathodes could achieve higher capacity compared with organic-based electrolyte Li–O_2 and Li–air batteries because the solid-state air cathode minimizes the O_2-transport limit. However, the energy output of the solid-state Li–air battery was lower than that of the solid-state Li–O_2 battery, resulting from H_2O and CO_2 contamination. It was confirmed from the cycling performance under pure O_2 that the side reaction of SP with Li_2O_2 caused the accumulation of Li_2CO_3, resulting in the loss of carbon. We believe that the poor cycling performance of the solid-state Li–air battery came from the combined impact of the formation of carbonate formed from CO_2 contamination and the loss of carbon from a side reaction. It was hypothesized that H_2O and CO_2 contamination played a major role; however, the cycling performance of the solid-state Li–air battery was not further deteriorated under the circumstance of limiting the capacity to a higher value of 1000 mA h g^{-1} (Figure S8 in the SI), which was similar to the performance in which the capacity was fixed to 500 mA h g^{-1} (Figure 6b). It was deduced that the stability of carbon greatly affected the cycling performance of the solid-state Li–O_2/air battery; maybe the cycling performance could be improved by introducing more stable cathode materials (TiC or nanoporous gold) or using another effective approach.[37,38] Along with carbon, the stability of other materials (the binder, current collector, and so on) also requires meticulous care and attention in the future; maybe the development of a binderless cathode is a better choice.[39] In our case, the proposed Li–O_2/air battery provided a promising approach to achieving practical application, but the stability of carbon is a key factor in limiting the cycling performance.

4. CONCLUSION

In conclusion, the results demonstrate that the proposed Li–O_2/air battery could successfully work under pure O_2 and ambient air and achieved high capacity. LATP was stable during cycling and avoided the decomposition and volatilization problems that conventional organic electrolytes faced; the porous air cathode provided a sufficient O_2-transport channel, facilitating the achievement of a high discharge capacity without using a special discharge mechanism (intermittent operation) or introducing a catalyst or functionalized carbon material. The first discharge capacity under O_2 or ambient air was 14192 or 7869 mA h g^{-1}, which was about 4 or 17 times that of the TEGDME-based electrolyte Li–O_2/air battery, respectively, at the current density of 100 mA g^{-1}. In addition, the fabrication method was simple. Considering the instability of SP, in the future, we should develop more stable carbon material or other material to improve the cycling performance.

■ ASSOCIATED CONTENT

Supporting Information

Detailed battery assembly, background experiment, SEM images of the discharge products, a comparison of two kinds of Li–O_2 batteries, and XPS and EIS results. This material is available free of charge via the Internet at http://pubs.acs.org.

■ AUTHOR INFORMATION

Corresponding Author

*E-mail: ygchen60@aliyun.com. Tel: +86 28 85407335. Fax: +86 28 85466916.

Notes

The authors declare no competing financial interest.

■ ACKNOWLEDGMENTS

This research was supported by the Synergistic Innovative Joint Foundation of AEP–SCU (Grant 0082604132222) and science and technology innovation "young plant project" of Sichuan Province (Grant 20132083).

■ REFERENCES

(1) Armand, M.; Tarascon, J. M. Building Better Batteries. *Nature* **2008**, *451*, 652–657.

(2) Wang, Y.; He, P.; Zhou, H. A Lithium–Air Capacitor–Battery Based on a Hybrid Electrolyte. *Energy Environ. Sci.* **2011**, *4*, 4994–4999.

(3) Abraham, K. M.; Jang, Z. A Polymer Electrolyte-Based Rechargeable Lithium/Oxygen Battery. *J. Electrochem. Soc.* **1996**, *143*, 1–5.

(4) Bruce, P. G.; Freunberger, S. A.; Hardwick, L. J.; Tarascon, J. M. Li–O_2 and Li–S Batteries with High Energy Storage. *Nat. Mater.* **2012**, *11*, 19–29.

(5) Jung, H. G.; Hassoun, J.; Park, J. B.; Sun, Y. K.; Scrosati, B. An Improved High-Performance Lithium–Air Battery. *Nat. Chem.* **2012**, *4*, 579–585.

(6) Read, J. Characterization of the Lithium/Oxygen Organic Electrolyte Battery. *J. Electrochem. Soc.* **2002**, *149*, A1190–A1195.

(7) Zhu, D.; Zhang, L.; Song, M.; Wang, X.; Mi, R.; Liu, H.; Mei, J.; Lau, L. W. M.; Chen, Y. Intermittent Operation of the Aprotic Li–O_2 Battery: the Mass Recovery Process Upon Discharge Interval. *J. Solid State Electrochem.* **2013**, *17*, 2539–2544.

(8) Zhu, D.; Zhang, L.; Song, M.; Wang, X.; Chen, Y. In Situ Formed Pd Nanolayer as a Bifunctional Catalyst for Li–Air Battery in Ambient or Simulated Air. *Chem. Commun.* **2013**, *49*, 9573–9575.

(9) McCloskey, B. D.; Scheffler, R.; Speidel, A.; Bethune, D. S.; Shelby, R. M.; Luntz, A. C. On the Efficacy of Electrocatalysis in Nonaqueous Li–O_2 Batteries. *J. Am. Chem. Soc.* **2011**, *133*, 18038–18041.

(10) Bryantsev, V. S.; Blanco, M. Computational Study of the Mechanisms of Superoxide-Induced Decomposition of Organic Carbonate-Based Electrolytes. *J. Phys. Chem. Lett.* **2011**, *2*, 379–383.

(11) Freunberger, S. A.; Chen, Y.; Peng, Z.; Griffin, J. M.; Hardwick, L. J.; Bardé, F.; Novák, P.; Bruce, P. G. Reactions in the Rechargeable Lithium–O_2 Battery with Alkyl Carbonate Electrolytes. *J. Am. Chem. Soc.* **2011**, *133*, 8040–8047.

(12) McCloskey, B. D.; Bethune, D. S.; Shelby, R. M.; Girishkumar, G.; Luntz, A. C. Solvents' Critical Role in Nonaqueous Lithium–Oxygen Battery Electrochemistry. *J. Phys. Chem. Lett.* **2011**, *2*, 1161–1166.

(13) Freunberger, S. A.; Chen, Y.; Drewett, N. E.; Hardwick, L. J.; Bardé, F.; Bruce, P. G. The Lithium–Oxygen Battery with Ether-Based Electrolytes. *Angew. Chem., Int. Ed.* **2011**, *50*, 8609–8613.

(14) McCloskey, B. D.; Speidel, A.; Scheffler, R.; Miller, D. C.; Viswanathan, V.; Hummelshøj, J. S.; Nørskov, J. K.; Luntz, A. C. Twin Problems of Interfacial Carbonate Formation in Nonaqueous Li–O_2 Batteries. *J. Phys. Chem. Lett.* **2012**, *3*, 997–1001.
(15) Imanishi, N.; Hasegawa, S.; Zhang, T.; Hirano, A.; Takeda, Y.; Yamamoto, O. Lithium Anode for Lithium–Air Secondary Batteries. *J. Power Sources* **2008**, *185*, 1392–1397.
(16) Zhou, H.; Wang, Y.; Li, H.; He, P. The Development of a New Type of Rechargeable Batteries Based on Hybrid Electrolytes. *ChemSusChem* **2010**, *3*, 1009–1019.
(17) Zhang, T.; Zhou, H. A Reversible Long-Life Lithium–Air Battery in Ambient Air. *Nat. Commun.* **2013**, *4*, 1–7.
(18) Kitaura, H.; Zhou, H. Electrochemical Performance and Reaction Mechanism of All-Solid-State Lithium–Air Batteries Composed of Lithium, $Li_{1+x}Al_yGe_{2-y}(PO_4)_3$ Solid Electrolyte and Carbon Nanotube Air Electrode. *Energy Environ. Sci.* **2012**, *5*, 9077–9084.
(19) Zhang, T.; Imanishi, N.; Takeda, Y.; Yamamoto, O. Aqueous Lithium/Air Rechargeable Batteries. *Chem. Lett.* **2011**, *40*, 668–673.
(20) Kichambare, P.; Rodrigues, S.; Kumar, J. Mesoporous Nitrogen-Doped Carbon–Glass Ceramic Cathodes for Solid-State Lithium–Oxygen Batteries. *ACS Appl. Mater. Interfaces* **2012**, *4*, 49–52.
(21) Kitaura, H.; Zhou, H. Electrochemical Performance of Solid-State Lithium–Air Batteries Using Carbon Nanotube Catalyst in the Air Electrode. *Adv. Energy Mater.* **2012**, *2*, 889–894.
(22) Wang, Y.; Zhou, H. To Draw an Air Electrode of a Li–Air Battery by Pencil. *Energy Environ. Sci.* **2011**, *4*, 1704–1707.
(23) Narváez-Semanate, J. L.; Rodrigues, A. C. M. Microstructure and Ionic Conductivity of $Li_{1+x}Al_xTi_{2-x}(PO_4)_3$ NASICON Glass–Ceramics. *Solid State Ionics* **2010**, *181*, 1197–1204.
(24) Best, A. S.; Newman, P. J.; MacFarlane, D. R.; Nairn, K. M.; Wong, S.; Forsyth, M. Characterisation and Impedance Spectroscopy of Substituted $Li_{1.3}Al_{0.3}Ti_{1.7}(PO_4)_{3-x}(ZO_4)_x$ (Z = V, Nb) Ceramics. *Solid State Ionics* **1999**, *126*, 191–196.
(25) Xu, X.; Wen, Z.; Yang, X.; Zhang, J.; Gu, Z. High Lithium Ion Conductivity Glass–Ceramics in Li_2O–Al_2O_3–TiO_2–P_2O_5 from Nanoscaled Glassy Powders by Mechanical Milling. *Solid State Ionics* **2006**, *177*, 2611–2615.
(26) Zhang, T.; Imanishi, N.; Hasegawa, S.; Hirano, A.; Xie, J.; Takeda, Y.; Yamamoto, O.; Sammes, N. Li/Polymer Electrolyte/Water Stable Lithium-Conducting Glass Ceramics Composite for Lithium–Air Secondary Batteries with an Aqueous Electrolyte. *J. Electrochem. Soc.* **2008**, *155*, A965–A969.
(27) Débart, A.; Paterson, A. J.; Bao, J.; Bruce, P. G. α-MnO_2 Nanowires: A Catalyst for the O_2 Electrode in Rechargeable Lithium Batteries. *Angew. Chem., Int. Ed.* **2008**, *47*, 4521–4524.
(28) Xu, J.; Xu, D.; Wang, Z.; Wang, H.; Zhang, L.; Zhang, X. Synthesis of Perovskite-Based Porous $La_{0.75}Sr_{0.25}MnO_3$ Nanotubes as a Highly Efficient Electrocatalyst for Rechargeable Lithium–Oxygen Batteries. *Angew. Chem., Int. Ed.* **2013**, *52*, 3887–3890.
(29) Lu, Y. C.; Xu, Z.; Gasteiger, H. A.; Chen, S.; Kimberly, H. S.; Yang, S. H. Platinum Gold Nanoparticles: A Highly Active Bifunctional Electrocatalyst for Rechargeable Lithium–Air Batteries. *J. Am. Chem. Soc.* **2010**, *132*, 12170–12171.
(30) Xu, J.; Wang, Z.; Xu, D.; Zhang, L.; Zhang, X. Tailoring Deposition and Morphology of Discharge Products Towards High-Rate and Long-Life Lithium–Oxygen Batteries. *Nat. Commun.* **2013**, *4*, 1–10.
(31) Jung, H. G.; Jeong, Y. S.; Park, J. B.; Sun, Y. K.; Scrosati, B.; Lee, Y. J. Ruthenium-Based Electrocatalysts Supported on Reduced Graphene Oxide for Lithium–Air Batteries. *ACS Nano* **2013**, *7*, 3532–3539.
(32) Han, X.; Hu, Y.; Yang, J.; Cheng, F.; Chen, J. Porous Perovskite $CaMnO_3$ as Electrocatalyst for Rechargeable Li–O_2 Batteries. *Chem. Commun.* **2014**, *50*, 1497–1499.
(33) Li, Q.; Xu, P.; Zhang, B.; Tsai, H.; Wang, J.; Wang, H. L.; Wu, G. One-Step Synthesis of Mn_3O_4/Reduced Graphene Oxide Nanocomposites for Oxygen Reduction in Nonaqueous Li–O_2 Batteries. *Chem. Commun.* **2013**, *49*, 10838–10840.
(34) Chowdari, B. V. R.; RAO, R. G. V. S.; Lee, G. Y. H. XPS and Ionic Conductivity Studies on Li_2O–Al_2O_3–(TiO_2 or GeO_2)–P_2O_5 Glass–Ceramics. *Solid State Ionics* **2000**, *136–137*, 1067–1075.
(35) Thotiyl, M. M. O.; Freunberger, S. A.; Zhang, P.; Bruce, P. G. The Carbon Electrode in Nonaqueous Li–O_2 Cells. *J. Am. Chem. Soc.* **2013**, *135*, 494–500.
(36) Gowda, S. R.; Brunet, A.; Wallraff, G. M.; McCloskey, B. D. Implications of CO_2 Contamination in Rechargeable Nonaqueous Li–O_2 Batteries. *J. Phys. Chem. Lett.* **2013**, *4*, 276–279.
(37) Thotiyl, M. M. O.; Freunberger, S. A.; Peng, Z.; Chen, Y.; Liu, Z.; Bruce, P. G. A Stable Cathode for the Aprotic Li–O_2 Battery. *Nat. Mater.* **2013**, *12*, 1050–1056.
(38) Shui, J.; Du, F.; Xue, C.; Li, Q.; Dai, L. Vertically Aligned N-Doped Coral-like Carbon Fiber Arrays as Efficient Air Electrodes for High-Performance Nonaqueous Li–O_2 Batteries. *ACS Nano* **2014**, *8*, 3015–3022.
(39) Nelson, R.; Kosivi, J.; Weatherspoon, M. H.; Kalu, E. E.; Zheng, J. P. Impedance Behavior of Binderless Ni–Mo Composite Oxide Cathode for a Li–O_2 Battery via Impedance Spectroscopy. *ECS Trans.* **2014**, *58*, 15–20.